Digital Signal Processing 71 (2017) 61–68

Contents lists available at ScienceDirect

Digital Signal Processing

www.elsevier.com/locate/dsp

TOA source localization and DOA estimation algorithms using prior distribution for calibrated source

Chee-Hyun Park, Joon-Hyuk Chang *

School of Electronic Engineering, Hanyang University, Seoul, 133-791, Republic of Korea

ARTICLE INFO

Article history:
Available online 11 September 2017

Keywords:
Expectation maximization (EM)
Space-alternating generalized expectation–maximization (SAGE)
Cramér–Rao lower bound (CRLB)
Position estimation
Time-of-arrival
Prior distribution

ABSTRACT

This paper presents an *a priori* probability density function (pdf)-based time-of-arrival (TOA) source localization algorithms. Range measurements are used to estimate the location parameter for TOA source localization. Previous information on the position of the calibrated source is employed to improve the existing likelihood-based localization method. The cost function where the prior distribution was combined with the likelihood function is minimized by the adaptive expectation maximization (EM) and space-alternating generalized expectation–maximization (SAGE) algorithms. The variance of the prior distribution does not need to be known *a priori* because it can be estimated using Bayes inference in the proposed adaptive EM algorithm. Note that the variance of the prior distribution should be known in the existing three-step WLS method [1]. The resulting positioning accuracy of the proposed methods was much better than the existing algorithms in regimes of large noise variances. Furthermore, the proposed algorithms can also effectively perform the localization in line-of-sight (LOS)/non-line-of-sight (NLOS) mixture situations.

1. Introduction

The aim of localization is to find a geometrical point of intersection using measurements from each receiver, based on the time difference of arrival (TDOA), the time of arrival (TOA), or the angle of arrival (AOA). Point source localization has been a popular issue for research in radar, sonar, global positioning system (GPS), and telecommunication fields [2–5]. A Taylor-series maximum likelihood (ML) method was employed to find the location of the target [2]. A closed-form TDOA-based positioning algorithm that reached the Cramér–Rao lower bound (CRLB) under sufficiently small noise conditions was proposed in [3]. The bias reduction source localization algorithm was devised to attenuate the bias due to the nonlinearity of the transformed measurements [4]. A shrinkage estimation-based localization approach was investigated to improve the mean square error (MSE) performance in the threshold regimes [5].

In GPS systems, differential calibration (DC) has been utilized to mitigate the effects of uncertainties in satellite positions caused by satellite environments. The calibrated source-based positioning method was introduced by applying the DC technique to the source localization [1], [6–9]. The DC technique was analyzed and an algebraic form of the solution was proposed and compared with the DC method and CRLB [6]. That approach considers the use of a single calibrated source whose position is known exactly, to improve the source localization accuracy in the presence of random sensor position errors. This algorithm was shown analytically to reach the CRLB for distant sources at sufficiently high signal-to-noise ratio (SNR) condition. In an extension of the results of [6], a closed-form solution was proposed for the situation where the exact position of the calibrated source is not known and the localization accuracy of this solution was compared with the conventional algorithm and CRLB [1]. The difference from [6] is that [1] modeled the position of the calibrated source as the Gaussian distribution model. The statistics of the position errors in both the receiving sensors and the calibrated emitter are exploited to come up with an algebraic closed-form solution. The solution is shown analytically to achieve the CRLB accuracy under some mild conditions. Non-causal radar-transmit beamforming was utilized to calibrate a physically large over-the-horizon radar [7]. The problem of locating multiple disjoint sources from the TDOA and frequency difference of arrival (FDOA) measurements was dealt with when the sensor locations were subject to random errors [8]. Also, the calibrated source position was assumed to follow the Gaussian distribution in [8]. It is found that when sensor location errors are present, joint source localization outperforms locating the sources

* Corresponding author.
E-mail address: jchang@hanyang.ac.kr (J.-H. Chang).

http://dx.doi.org/10.1016/j.dsp.2017.09.002
1051-2004/

separately in terms of significantly improved localization accuracy. On the other hand, in the absence of sensor location errors, locating multiple disjoint sources together and individually yielded the same performance. The optimum placement of the calibrated source was investigated by improving the Fisher information matrix (FIM) of the source location estimate in [9]. [9] defines the optimum calibration position to be the one that yields the source location FIM whose difference with those from all other positions to be positive definite (PD). Furthermore, [9] shows that the optimum calibration position is the unknown source position under certain situations such as identical and independent (IID) or very significant sensor position errors relative to the measurement noise and proposes a suboptimum calibrated emitter positioning criterion that indeed outperforms the closest to unknown source placement strategy.

The accuracy of the TOA source localization method is satisfactory in the LOS noise environments. However, in case of the positioning in indoor or urban areas, the localization performance of the LOS-based positioning method was severely degraded due to the multipath effects. To address these problems, robust localization methods were proposed [10–15]. The joint maximum *a posteriori*-ML (JMAP-ML) method was adopted by modeling the LOS–NLOS error distribution as a Gaussian mixture distribution [10]. Huber's M-estimate was applied to determine the position of the GPS and orthogonal transformations were used to guarantee the numerical stability of the method [11]. The least median squares (LMedS) estimator was employed to tackle the problems caused by the outliers [12], [13]. A weighted least squares (WLS) approach that exploits the statistics of multipath components was developed and small weights were given to the measurements which are likely to be biased [14]. However, the M- and LMedS estimators have the disadvantage that their computational complexity is relatively high. To overcome this problem, the closed-form α-trimmed mean and Hodges–Lehmann estimator were utilized for the localization of the source in the NLOS environments [15].

The motivation behind this paper is as follows. The distribution of the position parameters of the calibrated source can be modeled as a normal distribution [1], [6]. When this prior distribution is combined with the likelihood function, the localization performance can be improved drastically under low SNR conditions. The adaptive EM and space-alternating generalized expectation maximization (SAGE) based approaches are utilized during the minimization of the risk function [16–20]. The novelty of this paper is to divide the position of the calibrated source into two components, i.e., the first is the location of the source and the second is the remaining parameter to be estimated. Then, the unknown parameters are obtained in a sequential manner. Furthermore, the variance of the prior distribution does not need to be known *a priori* because it can be determined using Bayes inference in the proposed adaptive EM algorithm. Note that the variance of the prior distribution should be known in the existing three-step WLS method [1]. The proposed solution of this paper is the weighted sum of the estimate from the likelihood function and solution from the prior distribution. That is, as the variance in the measurement noise increases, the weight for the estimate from the prior probability density function (pdf) becomes relatively larger.

The rest of this paper is organized as follows. Section 2 explains the problem formulation to be solved in this paper. Section 3 provides details related to the proposed localization methods including the adaptive EM- and SAGE-based approaches. Section 4 evaluates the estimation performances of the proposed methods via the simulation results including a comparison with the existing methods and CRLB. Finally, Section 5 presents the conclusion.

2. Problem formulation

2.1. Line-of-sight (LOS) case

LOS situations occur when there is an unobstructed path between the transmitter and receiver. The measurement equation is first represented with an added noise component as follows:

$$\begin{aligned} r_i &= d_i + n_i \\ &= \sqrt{(x - x_i)^2 + (y - y_i)^2} + n_i \end{aligned} \tag{1}$$

where $n_i \sim N(0, \sigma_i^2)$, $i = 1, 2, \cdots, M$, with M denoting the number of sensors. We assumed that the noise components of the range measurements were independent. Note that $[x\ y]^T$ is the true position of the source and $[x_i\ y_i]^T$ is the position of the ith sensor. Throughout this paper, a lowercase boldface letter denotes a vector, an uppercase boldface letter indicates a matrix and the superscript T and H signify the vector/matrix transpose and conjugate transpose, respectively.

2.2. Line-of-sight (LOS)/non-line-of-sight (NLOS) mixture case

LOS/NLOS mixture scenarios occur when there is an obstruction between the transmitter and receiver. This is often the case in indoor environments and outdoor situations such as urban areas. In the LOS/NLOS mixture source localization context, the measurement equation is represented as

$$r_{i,j} = d_i + n_{i,j} = \sqrt{(x - x_i)^2 + (y - y_i)^2} + n_{i,j}, \tag{2}$$

where $n_{i,j} \sim (1 - \epsilon)N(0, \sigma_1^2) + \epsilon N(\mu_2, \sigma_2^2)$, $i = 1, 2, ..., M$, $j = 1, 2, ..., P$ with P denoting the number of samples in the ith sensor [21–23]. Also, $r_{i,j}$ is the measured distance between the source and the ith sensor at the jth sampling. The measurement noise $n_{i,j}$ is modeled as a Gaussian mixture distribution in which the LOS noise is distributed according to $N(0, \sigma_1^2)$ with a probability $(1 - \epsilon)$ and the NLOS noise distributed by $N(\mu_2, \sigma_2^2)$ with a probability of ϵ. We assumed that the statistics of the inlier can be obtained, but the mean and variance of the outlier distribution is unknown. Here, ϵ $(0 \le \epsilon \le 1)$ is the contamination ratio (i.e., fraction of contamination), which is a small number (typically smaller than 0.1) [21–23]. In this work, the LOS/NLOS mixture state is divided into the LOS and LOS/NLOS state. The LOS state denotes the case where the contamination ratio is zero $(\varepsilon = 0)$ and LOS/NLOS state is the condition in which $0 < \varepsilon \le 1$. Therefore, sensors always exist in the LOS or LOS/NLOS conditions. The purpose of this paper is to find the source position for which the MSE of the position estimate is minimized.

3. Proposed localization method

It is well known that the performance of the estimation method that uses the prior information can be improved in low SNR conditions or small sample environments compared to the approaches not using *a priori* information. To enhance the estimation performance of the existing positioning method, we utilized a prior pdf for the calibrated source location.

3.1. Localization algorithm using the prior PDF of the calibrated source position

3.1.1. Adaptive EM algorithm

In this section, we develop an algorithm based on an adaptive EM approach for which the variance in the prior pdf is determined by Bayes inference. Note that this work is referred to as

the adaptive EM method because the variance of the prior pdf for the calibrated source position is estimated by the adaptive EM procedure. The complete data log-likelihood concatenating *a priori* pdf of the calibrated source position is represented as follows:

$$\begin{aligned} l(\mathbf{x},\boldsymbol{\alpha},\sigma_c^2;\mathbf{r},\mathbf{x}_c) = &-\frac{M}{2}\ln 2\pi - \frac{M}{2}\ln\sigma_m^2 \\ &- \frac{1}{2\sigma_m^2}(\mathbf{r}-\mathbf{d}(\mathbf{x}))^T(\mathbf{r}-\mathbf{d}(\mathbf{x})) \\ &- \frac{L}{2}\ln 2\pi - \frac{L}{2}\ln\sigma_c^2 \\ &- \frac{1}{2\sigma_c^2}(\mathbf{x}_c-\mathbf{x}-\boldsymbol{\alpha})^T(\mathbf{x}_c-\mathbf{x}-\boldsymbol{\alpha}) \end{aligned} \tag{3}$$

where $\mathbf{r} = [r_1 \cdots r_M]^T$,

$$\mathbf{d}(\mathbf{x}) = [d_1(\mathbf{x}) \cdots d_M(\mathbf{x})]^T, \quad d_i(\mathbf{x}) = \sqrt{(x-x_i)^2+(y-y_i)^2},$$

σ_m^2 is the variance of the range measurement, σ_c^2 is the variance of the prior pdf for the calibrated source position, $\mathbf{x}_c$ is the prior which denotes the Cartesian coordinates of the calibrated source defined as $[x_c, y_c]^T$, $\mathbf{x} = [x, y]^T$ is the true position of the source, $\boldsymbol{\alpha} = E[\mathbf{x}_c] - \mathbf{x}$ and L is the dimension of $\mathbf{x}_c$. The prior $(\mathbf{x}_c)$ is modeled as the normal distribution, whose mean is $\mathbf{x}+\boldsymbol{\alpha}$ and variance is σ_c^2 ([1], [6]), for the convenience of the algorithmic development. Substituting $\mathbf{d}(\mathbf{x}^{(p)}) + \mathbf{D}(\mathbf{x}-\mathbf{x}^{(p)})$ into $\mathbf{d}(\mathbf{x})$ using a Taylor-series and rearranging the terms yields the following:

$$\begin{aligned} l(\mathbf{x},\boldsymbol{\alpha},\sigma_c^2;\mathbf{r},\mathbf{x}_c) = &-\frac{M}{2}\ln 2\pi - \frac{M}{2}\ln\sigma_m^2 \\ &- \frac{1}{2\sigma_m^2}(\mathbf{r}' - 2\mathbf{x}^T\mathbf{D}^T\mathbf{r}' + \mathbf{x}^T\mathbf{D}^T\mathbf{D}\mathbf{x}) \\ &- \frac{L}{2}\ln 2\pi - \frac{L}{2}\ln\sigma_c^2 \\ &- \frac{1}{2\sigma_c^2}(\mathbf{x}_c^T\mathbf{x}_c - 2(\mathbf{x}+\boldsymbol{\alpha})^T\mathbf{x}_c + (\mathbf{x}+\boldsymbol{\alpha})^T(\mathbf{x}+\boldsymbol{\alpha})) \end{aligned} \tag{4}$$

where $\mathbf{r}' = \mathbf{r} - \mathbf{d}(\mathbf{x}^{(p)}) + \mathbf{D}\mathbf{x}^{(p)}$ and $\mathbf{D}$ is the Jacobian matrix as given by

$$\mathbf{D} = \begin{pmatrix} \frac{\partial d_1(\mathbf{x})}{\partial x}|_{\mathbf{x}=\mathbf{x}^{(p)}} & \frac{\partial d_1(\mathbf{x})}{\partial y}|_{\mathbf{x}=\mathbf{x}^{(p)}} \\ \vdots & \vdots \\ \frac{\partial d_M(\mathbf{x})}{\partial x}|_{\mathbf{x}=\mathbf{x}^{(p)}} & \frac{\partial d_M(\mathbf{x})}{\partial y}|_{\mathbf{x}=\mathbf{x}^{(p)}} \end{pmatrix}.$$

The Q function is represented as follows:

$$\begin{aligned} \mathrm{Q}(\mathbf{x};\mathbf{x}^{(p)}) &= E[\ln p(\mathbf{r},\mathbf{x}_c;\mathbf{x},\boldsymbol{\alpha},\sigma_c^2) \mid \mathbf{r},\mathbf{x}^{(p)},\boldsymbol{\alpha}^{(p)},\sigma_c^{2\,(p)}] \\ &= C_1 + \frac{1}{\sigma_m^2}\mathbf{x}^T\mathbf{D}^T\mathbf{r}' - \frac{1}{2\sigma_m^2}\mathbf{x}^T\mathbf{D}^T\mathbf{D}\mathbf{x} \\ &\quad + \frac{1}{\sigma_c^2}(\mathbf{x}+\boldsymbol{\alpha})^T E[\mathbf{x}_c|\mathbf{r},\mathbf{x}^{(p)},\boldsymbol{\alpha}^{(p)},\sigma_c^{2\,(p)}] \\ &\quad - \frac{1}{2\sigma_c^2}(\mathbf{x}+\boldsymbol{\alpha})^T(\mathbf{x}+\boldsymbol{\alpha}) \end{aligned} \tag{5}$$

where C_1 is the constant irrespective of $\mathbf{x}$, $\boldsymbol{\alpha}$ and σ_c^2. From the Bayes theorem, $E[\mathbf{x}_c|\mathbf{r},\mathbf{x}^{(p)},\boldsymbol{\alpha}^{(p)},\sigma_c^{2\,(p)}] = \mathbf{x}^{(p)} + \boldsymbol{\alpha}^{(p)}$. Then, the parameters $\boldsymbol{\alpha}$ and $\mathbf{x}$ can be obtained by maximizing the Q function of (5) as follows:

$$\begin{aligned} \boldsymbol{\alpha}^{(p+1)} &= \mathbf{x}^{(p-1)} + \boldsymbol{\alpha}^{(p)} - \mathbf{x}^{(p)} \\ \mathbf{x}^{(p+1)} &= \mathbf{x}^{(p)} + \left(\frac{1}{\sigma_m^2}\mathbf{D}^T\mathbf{D} + \frac{1}{\sigma_c^{2\,(p)}}\mathbf{I}_M\right)^{-1} \\ &\quad \times \left(\frac{1}{\sigma_m^2}\mathbf{D}^T(\mathbf{r}-\mathbf{d}(\mathbf{x}^{(p)}) + \frac{1}{\sigma_c^{2\,(p)}}\boldsymbol{\alpha}^{(p)} - \frac{1}{\sigma_c^{2\,(p)}}\boldsymbol{\alpha}^{(p+1)}\right). \end{aligned} \tag{6}$$

Meanwhile, the variance of the prior pdf can be obtained using the Bayes inference approach. The variance of the prior pdf (σ_c^2) is assumed to have an inverse chi-square distribution, then $E[\frac{1}{\sigma_c^2}|\mathbf{r},\mathbf{x}^{(p)},\boldsymbol{\alpha}^{(p)},\sigma_c^{2\,(p)}] = [\frac{1}{L}(\mathbf{x}_c - (\mathbf{x}^{(p)}+\boldsymbol{\alpha}^{(p)}))^T(\mathbf{x}_c - (\mathbf{x}^{(p)}+\boldsymbol{\alpha}^{(p)}))]^{-1}$. Because $E[\mathbf{x}_c] = \mathbf{x}+\boldsymbol{\alpha}$, $E[\frac{1}{\sigma_c^2}|\mathbf{r},\mathbf{x}^{(p)},\boldsymbol{\alpha}^{(p)},\sigma_c^{2\,(p)}] \simeq [\frac{1}{L}(\mathbf{x}^{(p+1)} + \boldsymbol{\alpha}^{(p+1)} - (\mathbf{x}^{(p)}+\boldsymbol{\alpha}^{(p)}))^T(\mathbf{x}^{(p+1)} + \boldsymbol{\alpha}^{(p+1)} - (\mathbf{x}^{(p)} + \boldsymbol{\alpha}^{(p)}))]^{-1}$. The variance of the prior pdf was updated as described below:

$$\begin{aligned} \sigma_c^{2\,(p+1)} &= \frac{1}{L}(\mathbf{x}^{(p+1)} + \boldsymbol{\alpha}^{(p+1)} - \mathbf{x}^{(p)} - \boldsymbol{\alpha}^{(p)})^T \\ &\quad \times (\mathbf{x}^{(p+1)} + \boldsymbol{\alpha}^{(p+1)} - \mathbf{x}^{(p)} - \boldsymbol{\alpha}^{(p)}). \end{aligned} \tag{7}$$

3.1.2. SAGE algorithm

Since the EM algorithm suffers from a slow convergence rate, we apply the SAGE algorithm in this section, which may result in faster convergence than the EM method when one can sequentially update small groups of the elements of the parameter vector [18]. To obtain $\boldsymbol{\alpha}$, $\mathbf{x}$ and σ_c^2, the SAGE algorithm is accomplished by sequentially updating the parameter estimates as follows:

$$\begin{aligned} \boldsymbol{\alpha}^{(p+1)} &= \arg\max l(\mathbf{x}^{(p)},\boldsymbol{\alpha},\sigma_c^{2\,(p)}|\mathbf{q}_c^{(p)}) \\ \mathbf{x}^{(p+1)} &= \arg\max l(\mathbf{x},\boldsymbol{\alpha}^{(p+1)},\sigma_c^{2\,(p)}|\mathbf{q}_c^{(p)}) \\ \sigma_c^{2\,(p+1)} &= \arg\max l(\mathbf{x}^{(p+1)},\boldsymbol{\alpha}^{(p+1)},\sigma_c^2|\mathbf{q}_c^{(p)}) \end{aligned} \tag{8}$$

where $\mathbf{q}_c^{(p)} = E[\mathbf{x}_c|\mathbf{r},\mathbf{x}^{(p)},\boldsymbol{\alpha}^{(p)},\sigma_c^{2\,(p)}] = \mathbf{x}^{(p)} + \boldsymbol{\alpha}^{(p)}$. Then, the solution of (8) is obtained as follows:

$$\begin{aligned} \boldsymbol{\alpha}^{(p+1)} &= \mathbf{x}^{(p-1)} + \boldsymbol{\alpha}^{(p)} - \mathbf{x}^{(p)} \\ \mathbf{x}^{(p+1)} &= \mathbf{x}^{(p)} + \left(\frac{1}{\sigma_m^2}\mathbf{D}^T\mathbf{D} + \frac{1}{\sigma_c^{2\,(p)}}\mathbf{I}_M\right)^{-1} \\ &\quad \times \left(\frac{1}{\sigma_m^2}\mathbf{D}^T(\mathbf{r}-\mathbf{d}(\mathbf{x}^{(p)})) + \frac{1}{\sigma_c^{2\,(p)}}\boldsymbol{\alpha}^{(p)} - \frac{1}{\sigma_c^{2\,(p)}}\boldsymbol{\alpha}^{(p+1)}\right) \\ \sigma_c^{2\,(p+1)} &= \frac{1}{L}[\mathbf{q}_c^{(p)\,T}\mathbf{q}_c^{(p)} + \frac{L}{\frac{1}{\sigma_c^{2\,(p)}} + \frac{1}{\sigma_m^2}} - 2(\mathbf{x}^{(p+1)} + \boldsymbol{\alpha}^{(p+1)})^T\mathbf{q}_c^{(p)} \\ &\quad + (\mathbf{x}^{(p+1)} + \boldsymbol{\alpha}^{(p+1)})^T(\mathbf{x}^{(p+1)} + \boldsymbol{\alpha}^{(p+1)})]. \end{aligned} \tag{9}$$

3.2. Direction of arrival (DOA) estimation using the prior PDF for the DOA of the calibrated source

In this section, we derive the DOA estimation algorithm in which the prior pdf for the DOA of the calibrated source is utilized. The complete data log-likelihood combining the prior pdf for the DOA of the calibrated source is represented as follows [1], [6]:

$$\begin{aligned} l(\boldsymbol{\theta},\boldsymbol{\alpha},\sigma_c^2;\mathbf{x}(t),\boldsymbol{\theta}_c) = C - \ln|\mathbf{R}_\mathbf{x}| - \mathbf{x}(t)^H\mathbf{R}_\mathbf{x}^{-1}\mathbf{x}(t) \\ - \frac{1}{2\sigma_c^2}\{(\boldsymbol{\theta}_c - \boldsymbol{\theta} - \boldsymbol{\alpha})^T(\boldsymbol{\theta}_c - \boldsymbol{\theta} - \boldsymbol{\alpha})\}, \end{aligned} \tag{10}$$

where $\mathbf{x}(t) = \mathbf{A}\mathbf{s}(t) + \mathbf{n}(t)$ is the received signal vector, $\mathbf{A} = [\mathbf{a}(\theta_1)\cdots\mathbf{a}(\theta_L)]$, $\mathbf{a}(\theta_l) = [1 \quad e^{-\frac{i2\pi f_c}{\lambda}d\sin(\theta_l)} \cdots e^{-\frac{i2\pi f_c}{\lambda}(M-1)d\sin(\theta_l)}]^T$, λ is the wavelength of the propagating wave, f_c is the carrier frequency, d is the spacing between sensor elements, $\mathbf{n}(t)$ is the

complex measurement noise with zero mean, $\mathbf{s}(t)$ is the random complex signal with zero mean, $\mathbf{R_x} = \sigma_s^2 \mathbf{A}\mathbf{A}^H + \sigma_m^2 \mathbf{I}_M$ is the covariance matrix of the received signal, $\mathbf{I}_M$ is the $M \times M$ identity matrix, $\sigma_s^2 \mathbf{I}_L$ is the variance of $\mathbf{s}(t)$, L is the dimension of $\mathbf{s}(t)$, $\sigma_m^2 \mathbf{I}_M$ is the variance of the measurement noise, $\boldsymbol{\theta}_c$ is the *a priori* incident angle of the calibrated source, $\boldsymbol{\theta}$ are the true incident angles of the sources, $\boldsymbol{\alpha} = E[\boldsymbol{\theta}_c] - \boldsymbol{\theta}$, σ_c^2 is the variance of the prior pdf of the incident angle of the calibrated source and C is the constant irrespective of $\boldsymbol{\theta}, \boldsymbol{\alpha}$ and σ_c^2.

Then, Q function is found by taking the conditional expectation for the missing variable $\boldsymbol{\theta}_c$ given the incomplete data $\mathbf{x}(t)$ and current estimate $\boldsymbol{\theta}^{(p)}$ as follows:

$$\begin{aligned}
\mathrm{Q}(\boldsymbol{\theta}; \boldsymbol{\theta}^{(p)}) &= E[\ln p(\mathbf{x}(t), \boldsymbol{\theta}_c; \boldsymbol{\theta}, \boldsymbol{\alpha}, \sigma_c^2) \mid \mathbf{x}(t), \boldsymbol{\theta}^{(p)}] \\
&= C - \ln|\mathbf{R_x}| - \mathbf{x}(t)^H \mathbf{R_x}^{-1} \mathbf{x}(t) \\
&\quad + \frac{1}{\sigma_c^2} (\boldsymbol{\theta} + \boldsymbol{\alpha})^T E[\boldsymbol{\theta}_c \mid \mathbf{x}(t), \boldsymbol{\theta}^{(p)}] \\
&\quad - \frac{1}{2\sigma_c^2} \boldsymbol{\theta}^T \boldsymbol{\theta} - \frac{1}{\sigma_c^2} \boldsymbol{\alpha}^T \boldsymbol{\theta} \\
&= C - \ln|\mathbf{R_x}| - \mathbf{x}(t)^H \mathbf{R_x}^{-1} \mathbf{x}(t) \\
&\quad + \frac{1}{\sigma_c^2} (\boldsymbol{\theta} + \boldsymbol{\alpha})^T (\boldsymbol{\theta}^{(p)} + \boldsymbol{\alpha}^{(p)}) \\
&\quad - \frac{1}{2\sigma_c^2} \boldsymbol{\theta}^T \boldsymbol{\theta} - \frac{1}{\sigma_c^2} \boldsymbol{\alpha}^T \boldsymbol{\theta}. \qquad (11)
\end{aligned}$$

The parameter $\boldsymbol{\theta}$ is obtained by the Newton–Raphson algorithm as follows:

$$\boldsymbol{\theta}^{(p+1)} = \boldsymbol{\theta}^{(p)} - \rho \cdot \mathrm{Q}_{\boldsymbol{\theta}\boldsymbol{\theta}}^{-1} \mathrm{Q}_{\boldsymbol{\theta}} \qquad (12)$$

where ρ is the step size,

$$\begin{aligned}
\mathrm{Q}_{\boldsymbol{\theta}} &= \frac{\partial \mathrm{Q}(\boldsymbol{\theta}; \boldsymbol{\theta}^{(p)})}{\partial \boldsymbol{\theta}} \\
&= 2\mathrm{Re}(\mathrm{Diag}[\mathbf{G}^H \widehat{\mathbf{R}}_{\mathbf{x}} \mathbf{P}_{\mathbf{A}}^{\perp} \mathbf{E}]) + \frac{1}{\sigma_c^{2(p)}} (-\mathbf{u}_c^{(p)} + \boldsymbol{\theta}^{(p)} + \boldsymbol{\alpha}^{(p)}) \\
&= 2\mathrm{Re}(\mathrm{Diag}[\mathbf{G}^H \widehat{\mathbf{R}}_{\mathbf{x}} \mathbf{P}_{\mathbf{A}}^{\perp} \mathbf{E}]), \qquad (13)
\end{aligned}$$

$$\begin{aligned}
\mathrm{Q}_{\boldsymbol{\theta}\boldsymbol{\theta}} &= \frac{\partial \mathrm{Q}^2(\boldsymbol{\theta}; \boldsymbol{\theta}^{(p)})}{\partial^2 \boldsymbol{\theta}} \\
&= 2\widehat{\sigma_m^2} \mathrm{Re}[(\mathbf{E}^H \mathbf{P}_{\mathbf{A}}^{\perp} \mathbf{E}) \odot (\mathbf{G}^H \widehat{\mathbf{R}}_{\mathbf{x}} \mathbf{G})^T] + \frac{1}{\sigma_c^{2(p)}} \mathbf{I}_L \qquad (14)
\end{aligned}$$

where

$$\mathbf{u}_c^{(p)} = E[\boldsymbol{\theta}_c \mid \mathbf{x}(t), \boldsymbol{\theta}^{(p)}] = \boldsymbol{\theta}^{(p)} + \boldsymbol{\alpha}^{(p)},$$

$$\widehat{\mathbf{R}}_{\mathbf{x}} = \frac{1}{P} \sum_{n=1}^{P} \mathbf{x}(n) \mathbf{x}^H(n),$$

P is the number of snapshots, $\mathbf{P}_{\mathbf{A}}^{\perp} = \mathbf{I} - \mathbf{A}(\mathbf{A}^H \mathbf{A})^{-1} \mathbf{A}^H$, $\widehat{\sigma_m^2} = \frac{\mathrm{tr}[\mathbf{P}_{\mathbf{A}}^{\perp} \widehat{\mathbf{R}}_{\mathbf{x}}]}{P - L}$, $\mathbf{G} = \mathbf{A}[(\mathbf{A}^H \widehat{\mathbf{R}}_{\mathbf{x}} \mathbf{A})^{-1} - \widehat{\sigma_m^2} (\mathbf{A}^H \mathbf{A})^{-1}]$, $\odot$ is the component-wise product, and $\mathbf{E} = [\frac{\partial \mathbf{a}(\theta_1)}{\partial \theta_1} \cdots \frac{\partial \mathbf{a}(\theta_L)}{\partial \theta_L}]$ and σ_c^2 is found by the adaptive EM and SAGE methods in the same manner with the cases of the TOA localization.

4. Simulation results

4.1. Simulation settings

In this section, the MSE performance of the proposed localization method was compared with the conventional methods ([1], [2], [8]) and CRLB. The simulation setting is represented in Table 1. The MSE average was calculated as follows:

Table 1
Simulation settings.

Source location	located within a 2×2 km^2 region
Number of simulated sources	30
Number of Monte-Carlo simulation	200
Range measurement noise variance of each sensor	assumed to be identical
Number of sensors	7
Variance of the prior pdf (σ_c^2)	400 m^2

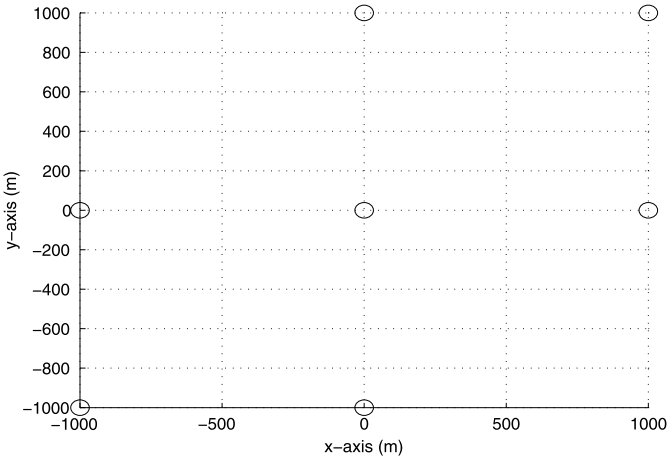

Fig. 1. Deployment of sensors.

$$\text{MSE average} = \frac{\sum_{i=1}^{I} \sum_{k=1}^{K} [(\widehat{x}^k(i) - x(i))^2 + (\widehat{y}^k(i) - y(i))^2]}{I \times K} \qquad (15)$$

where I is the total number of elements of the simulated source position set, K is the number of simulation runs, $\widehat{x}^k(i)$ and $\widehat{y}^k(i)$ are the estimated position coordinates of the source in the ith position set and kth iteration, and $x(i)$ and $y(i)$ indicate the ith true position of the source. The initial position of the proposed iterative method was selected randomly as a point on the circle of $(x^{\text{init}} - x)^2 + (y^{\text{init}} - y)^2 = 50^2$, where x, y are the true position coordinates of the source and x^{init}, y^{init} are the initial points of the iterative algorithms. The initial value for the variance of the calibration source position prior (σ_c^2) was $\sigma_c^2 + 200$, where σ_c^2 is the true variance of the prior pdf for the calibrated source position. The initial value of $\boldsymbol{\alpha}$ in the adaptive EM and SAGE algorithm was selected randomly as a point on the circle of $(\alpha_1^{\text{init}} - \alpha_1^{\text{o}})^2 + (\alpha_2^{\text{init}} - \alpha_2^{\text{o}})^2 = 100^2$, where α_1^{init}, α_2^{init} are the initial points of $\boldsymbol{\alpha}$ and α_1^{o}, α_2^{o} are the true values of $\boldsymbol{\alpha}$.

4.2. Simulation results

The resulting localization accuracy as a function of the variance of range measurement noise is given in Fig. 2 for the configuration shown in Fig. 1. The MSE averages of the proposed methods with the prior pdf were much better than the three-step WLS [1] and Taylor-series ML [2] algorithms in the regimes of large noise variances. Also, the proposed methods outperformed the CRLB in low SNR regimes. The MSE of the biased estimator can be smaller than the CRLB in low SNR regimes or for a small number of samples [24], [25]. The rationale of this observation is as follows. Let us assume the biased estimator as the shrinkage estimator because the shrinkage estimator is one among the biased estimators. The shrinkage factor is obtained as follows [24], [25]:

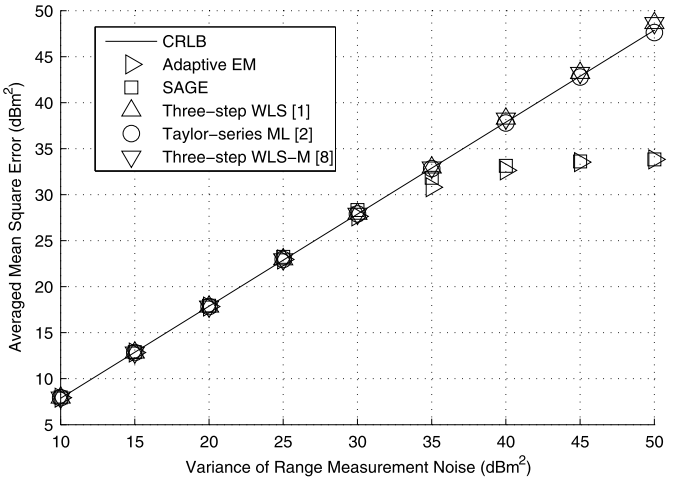

Fig. 2. Comparison of MSE averages of the proposed localization methods with that of the existing methods as a function of variance of range measurement noise.

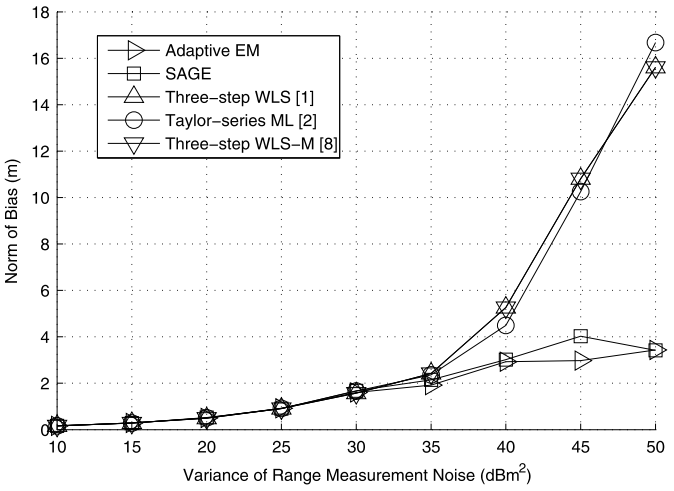

Fig. 3. Comparison of norm of bias of the proposed localization methods as a function of variance of range measurement noise.

$$m^s = \frac{(\widehat{\gamma}^e)^2}{(\widehat{\gamma}^e)^2 + \mathrm{var}[\widehat{\gamma}^e]} \tag{16}$$

where $\widehat{\gamma}^e$ is the efficient estimator for the true parameter γ, such as the LS or ML estimator. By using m^s, the shrinkage estimator is found as follows:

$$\widehat{\gamma}^s = m^s \cdot \widehat{\gamma}^e \tag{17}$$

where $\widehat{\gamma}^s$ turns out to be the multiplication of the shrinkage factor and the efficient estimator. Accordingly, it is discovered that the MSE can be reduced compared to the conventional unbiased estimator by appropriately selecting the shrinkage factor. Indeed, the MSE of the shrinkage estimator can be obtained as follows:

$$\mathrm{MSE}(\widehat{\gamma}^s) = \mathrm{var}(\widehat{\gamma}^s) + \mathrm{bias}^2(\widehat{\gamma}^s). \tag{18}$$

Then, (18) can be rewritten as

$$\mathrm{MSE}(\widehat{\gamma}^s) = (m^s)^2\mathrm{var}(\widehat{\gamma}^e) + (m^s - 1)^2\gamma^2. \tag{19}$$

This implies that the MSE is quantified in a fashion of the equation containing the shrinkage factor and thus can be smaller than that when using the unbiased optimal estimator by controlling the shrinkage factor. Specifically, the MSE of the shrinkage estimator can be adjusted to be smaller than that of the unbiased optimal estimator if $(m^s)^2\mathrm{var}(\widehat{\gamma}^e) + (1-m^s)^2\gamma^2 < \mathrm{var}(\widehat{\gamma}^e)$. When rearranging (19) for the shrinkage factor m^s, the MSE of the shrinkage estimator is smaller than that of the unbiased optimal estimator if the shrinkage factor lies within $\frac{\gamma^2 - \mathrm{var}(\widehat{\gamma}^e)}{\gamma^2 + \mathrm{var}(\widehat{\gamma}^e)} < m^s < 1$. Fig. 3 exhibits a comparison of the norm of bias of the localization methods and the norm of bias of the proposed algorithms was large in the low SNR regimes. The proposed position estimate is the weighted sum of the estimate from the log-likelihood function and the solution from the prior pdf. Namely, as the variance in the range measurement noise increases, the weight for the estimate from the prior pdf becomes relatively larger. The variance of the prior pdf for the calibrated source location does not need to be known *a priori* in the proposed methods because it is estimated in an iterative manner unlike the existing methods [1]. Fig. 4 shows the MSE averages as a function of number of sensors when the variance of range measurement noise was 40 dBm^2. The MSE averages decreased as the number of sensors increased and the performance of adaptive EM method was most superior. Fig. 5 illustrates the MSE averages as a function of variance of sensor position error when the variance of range measurement noise was -30 dBm^2. The localization performance was robust up

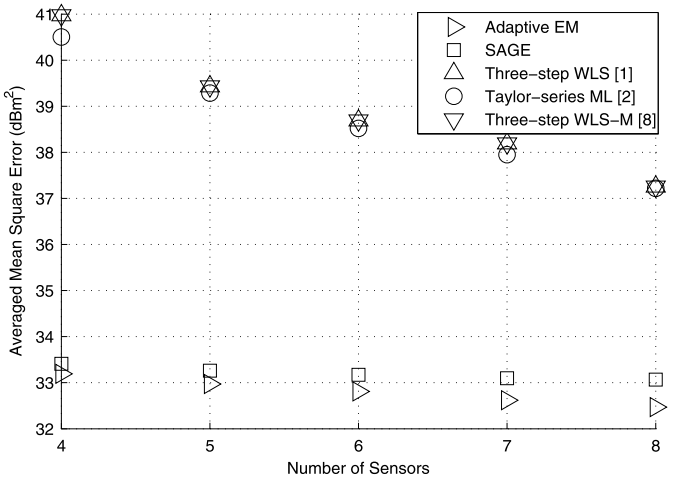

Fig. 4. MSE averages of the localization algorithms as a function of number of sensors.

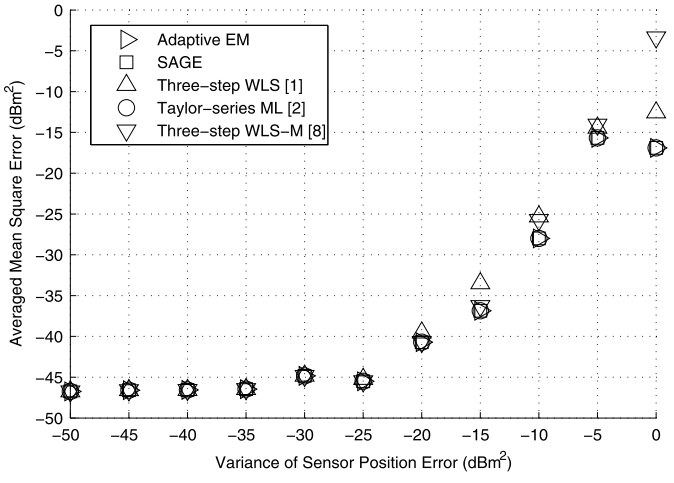

Fig. 5. MSE averages of the localization algorithms as a function of variance of sensor position error.

to approximately -25 dBm^2 of variance of sensor position noise. Fig. 6 shows the MSE averages as a function of variance of calibration noise when the variance of range measurement noise was 40 dBm^2. The MSE averages increased as the calibration noise in-

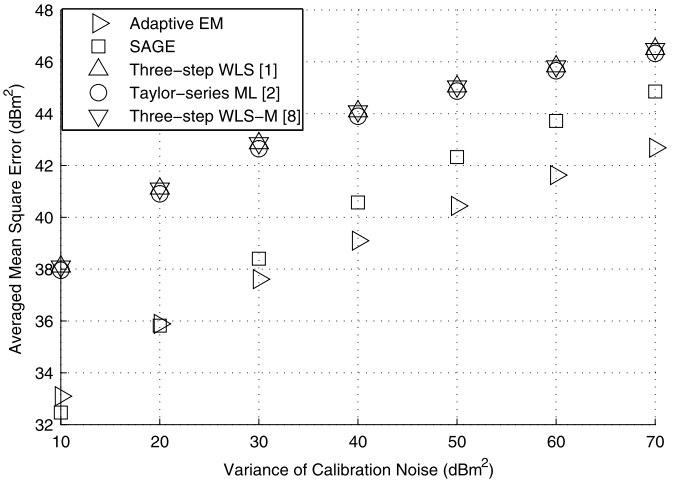

Fig. 6. MSE averages of the localization algorithms as a function of variance of calibration noise.

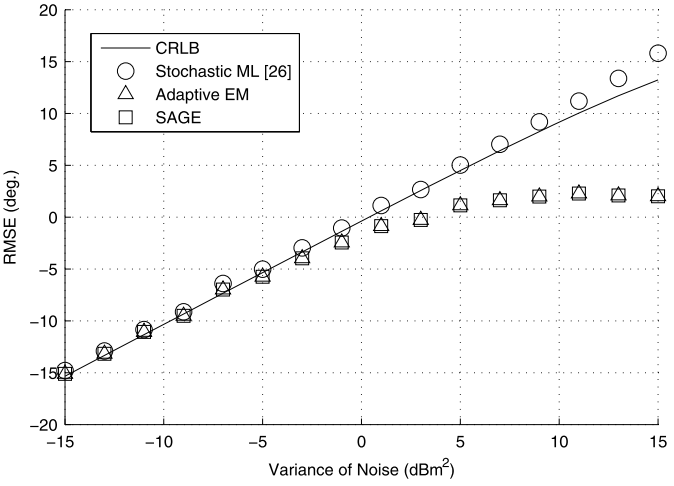

Fig. 7. MSE averages of the DOA estimation of the proposed algorithms using the DOA prior pdf of the calibrated source (DOA of source $= [\frac{\pi}{6}\ \frac{\pi}{3}\ \frac{4\pi}{5}]$).

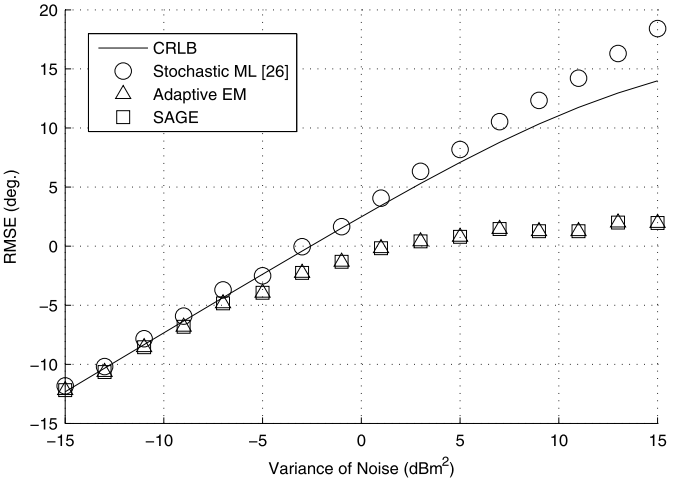

Fig. 8. MSE averages of the DOA estimation of the proposed algorithms using the DOA prior pdf of the calibrated source (DOA of source $= [\frac{\pi}{8}\ \frac{\pi}{4}\ \frac{2\pi}{3}]$).

creased and the performance of adaptive EM method was most superior. Also, Figs. 7 and 8 show the MSE average of DOA estimation as a function of the noise variances using the DOA prior pdf of the calibrated source. A uniform linear array (ULA) was

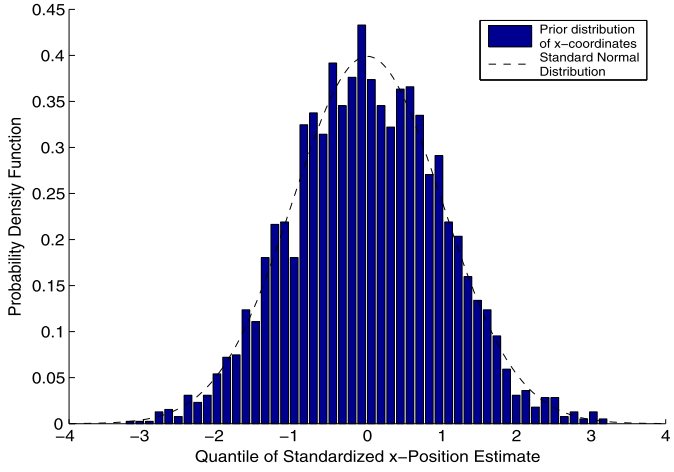

Fig. 9. Probability density function of prior (x-coordinates).

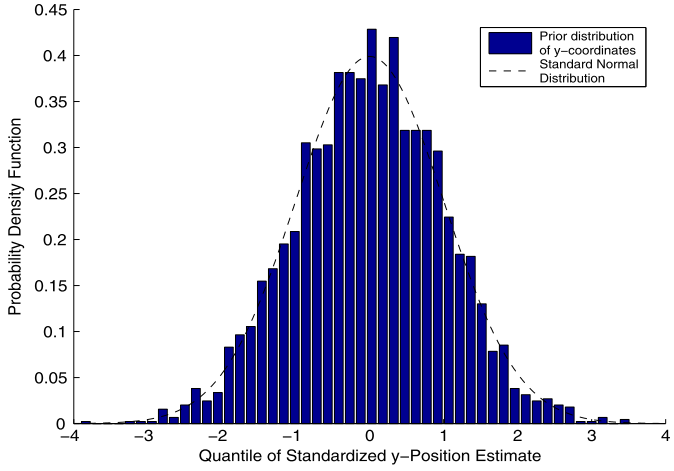

Fig. 10. Probability density function of prior (y-coordinates).

utilized and there were eight sensors at which the number of sources was assumed to be three and their DOAs were $\pi/6$, $\pi/3$ and $4\pi/5$ as in Fig. 7 and $\pi/8$, $\pi/4$ and $2\pi/3$ as in Fig. 8, respectively. The number of measurements was 40, the variance of the signal was 25 and $\sigma_c^2 = 0.01$ rad^2. The initial values of DOAs were $\boldsymbol{\theta}^o + 0.01 \times \mathbf{rn}$, where $\mathbf{rn} = [rn_1 \cdots rn_L]^T$, rn_l $(l = 1 \cdots L)$ is a random number with $N(0,\ 1)$, $\boldsymbol{\theta}^o$ was the true DOAs of the sources and the initial variance of the DOA prior pdf for the calibrated source was $\sigma_c^2 + 0.01$. The initial point of $\boldsymbol{\alpha}$ was selected as $\boldsymbol{\alpha}^o + 0.01 \times \mathbf{rn}$ and the step-size of the Newton–Raphson algorithm was 0.7, where $\boldsymbol{\alpha}^o$ is the true value of $\boldsymbol{\alpha}$. The MSE averages of the adaptive EM and SAGE approaches were superior to the stochastic ML [26] and CRLB because they employ an *a priori* DOA distribution for the calibrated source. Figs. 9 and 10 show the distribution of x, y coordinates of the prior and the prior location was obtained from the WLS method. The number of prior samples was 3000. As can be seen from Figs. 9 and 10, the distribution of prior was close to the standard normal distribution, which was explicitly confirmed by Kolmogorov–Smirnov (KS) test under the significant level of 5%. Furthermore, the adaptive EM and SAGE localization algorithms can be applied for robust localization. The measurement equation described in the Section 2.2 was utilized and the median for the measurements of each sensor was adopted as the observation in the robust localization procedure ((6), (9)) instead of $\mathbf{r} = [r_1 \cdots r_M]^T$. The contamination ratio (ε) was 20% and three sensors were the LOS/NLOS sensors in the simulation of the robust localization. Fig. 11 shows the MSE average as a function of the

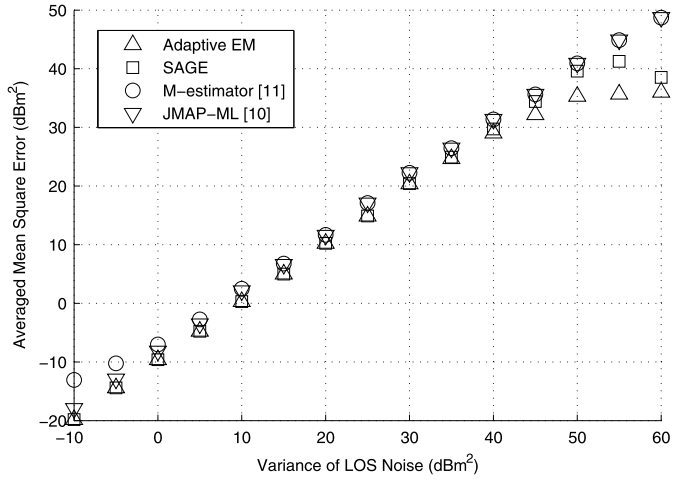

Fig. 11. MSE averages of the robust localization algorithms as a function of variance of LOS noise in the LOS/NLOS mixture environments.

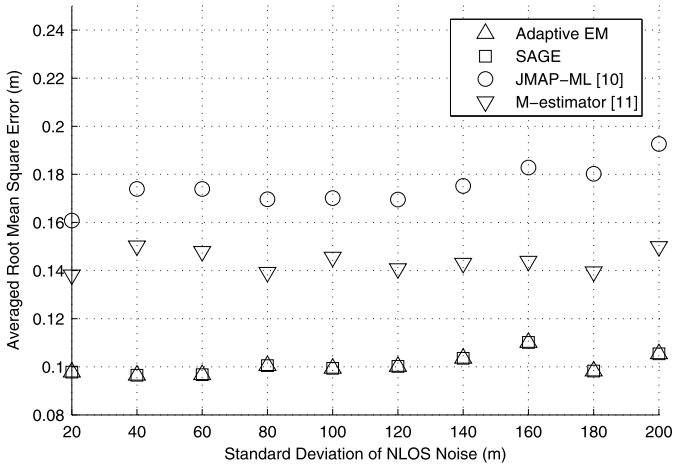

Fig. 12. MSE averages of the robust localization algorithms as a function of variance of NLOS noise in the LOS/NLOS mixture environments.

Table 2
Comparison of the computational complexity.

Algorithm	Computational complexity
Three-step WLS [1]	$O(NM^2) + O(N^2M) + O(N^3) + O(M^3)$
Adaptive EM	$I \times (O(N^3) + O(N^2M))$
SAGE	$I \times (O(N^3) + O(N^2M))$
Three-step WLS-M [8]	$L \times (O(NM^2) + O(N^2M) + O(N^3) + O(M^3))$

variance of the LOS noise. The MSE average of the proposed methods was superior to the existing algorithms and an increase in the MSE average resulted in a reduction in the large LOS noise regimes due to the aid of the calibrated source prior. Fig. 12 exhibits the MSE average of the robust localization methods as a function of the standard deviation of the NLOS noise and the proposed methods could effectively estimate the position of the source in the LOS/NLOS mixture environments as well.

Also, we compared the computational complexity of localization algorithms. Table 2 shows the computational complexity of the three-step WLS [1], three-step WLS-M [8] and proposed algorithms, where M is the number of sensors, N is the number of parameters, I is the iteration number and L is the number of calibrated sources. The computational complexity was dependent on the matrix inverse and multiplication operations because their computational load is higher than that of other operations.

5. Conclusions

The *a priori*-based TOA localization methods were developed, in which the proposed methods utilized the prior pdf from calibrated source position. The complete data log-likelihood which combines the log-likelihood and prior pdf was maximized using the adaptive EM and SAGE algorithms. The novelty of this paper is to partition the position of the calibrated source into two parts; one is the location of the source and the other is the remaining part to be estimated. Then, the unknown parameters are calculated sequentially. The variance of the prior distribution does not need to be known *a priori* unlike the existing three-step WLS method in which the variance of the prior distribution should be known. The MSE averages of the proposed methods were much smaller in the large noise variances regimes than that of the three-step WLS and Taylor-series ML methods. Also, the computational complexity of the proposed methods was compared. The localization performance of the proposed methods was improved as the number of sensors increased and was robust up to approximately -25 dBm^2 of the sensor position error. The proposed methods effectively performed the localization in LOS/NLOS mixture environments as well.

Acknowledgment

This research was supported by Basic Science Research Program through the National Research Foundation of Korea (NRF) funded by the MSIP (NRF-2017R1A2A1A17069651).

References

[1] L. Yang, K.C. Ho, Alleviating sensor position error in source localization using calibration emitters at inaccurate locations, IEEE Trans. Signal Process. 58 (1) (Jan. 2010) 67–83.
[2] D.J. Torrieri, Statistical theory of passive location systems, IEEE Trans. Aerosp. Electron. Syst. 20 (2) (Jun. 1983) 183–198.
[3] Y.T. Chan, K.C. Ho, A simple and efficient estimator for hyperbolic location, IEEE Trans. Signal Process. 42 (8) (May 1994) 1905–1915.
[4] K.C. Ho, Bias reduction for an explicit solution of source localization using TDOA, IEEE Trans. Signal Process. 60 (5) (May 2012) 2101–2114.
[5] C.H. Park, J.-H. Chang, Shrinkage estimation-based source localization with minimum mean squared error criterion and minimum bias criterion, Digit. Signal Process. 29 (Jun. 2014) 100–106.
[6] K.C. Ho, L. Yang, On the use of a calibration emitter for source localization in the presence of sensor position uncertainty, IEEE Trans. Signal Process. 56 (12) (Dec. 2008) 5758–5772.
[7] G.J. Frazer, Y.I. Abramovich, B.A. Johnson, MIMO based spatial calibration of OTHR transmit arrays, in: Proc. Radar Conference – Surveillance for a Safer World, Oct. 2009.
[8] J. Li, H. Pang, F. Guo, L. Yang, W. Jiang, Localization of multiple disjoint sources with prior knowledge on source locations in the presence of sensor location errors, Digit. Signal Process. 40 (May 2015) 181–197.
[9] Z. Ma, K.C. Ho, A study on the effects of sensor position error and the placement of calibration emitter for source localization, IEEE Trans. Wirel. Commun. 13 (10) (Oct. 2014) 5440–5452.
[10] Y. Feng, C. Fritsche, F. Gustafsson, A.M. Zoubir, EM- and JMAP-ML based joint estimation algorithms for robust wireless geolocation in mixed LOS/NLOS environments, IEEE Trans. Signal Process. 62 (1) (Jan. 2014) 168–182.
[11] X.-W. Chang, Y. Guo, Huber's M-estimation in relative GPS positioning: computational aspects, J. Geod. 79 (6) (Aug. 2005) 351–362.
[12] P.J. Rousseeuw, Least median of squares regression, Am. Stat. Assoc. 79 (388) (Dec. 1984) 871–880.
[13] Z. Li, W. Trappe, Y. Zhang, B. Nath, Robust statistical methods for securing wireless localization in sensor networks, in: Proc. of IEEE International Symposium on Information Processing in Sensor Networks (IPSN), Los Angeles, CA, Apr. 2005.
[14] I. Güvenç, C.C. Chong, F. Watanabe, H. Inamura, NLOS identification and weighted least-squares localization for UWB systems using multipath channel statistics, EURASIP J. Adv. Signal Process. (Jan. 2008) 271984.
[15] C.H. Park, S. Lee, J.-H. Chang, Robust closed-form time-of-arrival source localization based on α-trimmed mean and Hodges–Lehmann estimator under NLOS environments, Signal Process. 111 (Jun. 2015) 113–123.
[16] A.P. Dempster, N.M. Laird, D.B. Rubin, Maximum likelihood from incomplete data via the EM algorithm, J. R. Stat. Soc., Ser. B 39 (1) (1977) 1–38.

[17] T.K. Moon, The expectation–maximization algorithm, IEEE Signal Process. Mag. 13 (6) (Nov. 1996) 47–60.
[18] J.A. Fessler, A.O. Hero, Space-alternating generalized expectation–maximization algorithm, IEEE Trans. Signal Process. 42 (10) (Oct. 1994) 2664–2677.
[19] B.H. Fleury, M. Tschudin, R. Heddeergott, D. Dahlhaus, K.I. Pedersen, Channel parameter estimation in mobile radio environments using the SAGE algorithm, IEEE J. Sel. Areas Commun. 17 (3) (Mar. 1999) 434–450.
[20] F. Yang, J. Song, Y. Zhang, C. Pan, Z. Yang, SAGE-based estimation of doubly selective channel with an orthogonal polynomial model, Signal Process. 88 (Apr. 2008) 1061–1068.
[21] F. Gustafsson, F. Gunnarsson, Mobile positioning using wireless networks, IEEE Signal Process. Mag. (Jul. 2005) 41–53.
[22] U. Hammes, E. Wolsztynski, A.M. Zoubir, Robust tracking and geolocation for wireless networks in NLOS environments, IEEE J. Sel. Top. Signal Process. 3 (5) (Oct. 2009) 889–901.
[23] Y. Feng, C. Fritsche, F. Gustafsson, A.M. Zoubir, TOA-based robust wireless geolocation and Cramer–Rao lower bound analysis in harsh LOS/NLOS environments, IEEE Trans. Signal Process. 61 (9) (May 2013) 2243–2255.
[24] Y.C. Eldar, Uniformly improving the Cramér–Rao bound and maximum-likelihood estimation, IEEE Trans. Signal Process. 54 (8) (Aug. 2006) 2943–2956.
[25] B. Efron, Biased versus unbiased estimation, Adv. Math. 16 (3) (1975) 259–277.
[26] H.L.V. Trees, Optimum Array Processing: Part IV of Detection, Estimation and Modulation Theory, Wiley, 2012.

Chee-Hyun Park received the Ph.D. degree in electronics and computer engineering from Sungkyunkwan University, Suwon, South Korea, in 2011. From April 2011 to August 2012, he was with University of Wisconsin–Madison, Madison, WI, USA, as a Postdoctoral Fellow. Currently, he is a Research Professor with Hanyang University, Seoul, South Korea. His research interests include estimation theory particularly in signal processing, source localization, and array signal processing.

Joon-Hyuk Chang received the B.S. degree in electronics engineering from Kyungpook National University, Daegu, South Korea in 1998 and the M.S. and Ph.D. degrees in electrical engineering from Seoul National University, South Korea, in 2000 and 2004, respectively. From March 2000 to April 2005, he was with Netdus Corp., Seoul, as a chief engineer. From May 2004 to April 2005, he was with the University of California, Santa Barbara, in a postdoctoral position to work on adaptive signal processing and audio coding. In May 2005, he joined Korea Institute of Science and Technology, Seoul, as a Research Scientist to work on speech recognition. From August 2005 to February 2011, he was an assistant professor in the School of Electronic Engineering at Inha University, Incheon, South Korea. Currently, he is an associate professor in the School of Electronic Engineering at Hanyang University, Seoul, South Korea. His research interests are in speech coding, speech enhancement, speech recognition, audio coding, and adaptive signal processing. He is a senior member of IEEE. He is a winner of IEEE/IEEK IT young engineer of the year 2011. He is serving as Editor-in-chief of the Signal Processing Society Journal of the IEEK.